IEEE Access
Multidisciplinary ⋮ Rapid Review ⋮ Open Access Journal

Received April 21, 2019, accepted May 16, 2019, date of publication May 24, 2019, date of current version January 3, 2020.

*Digital Object Identifier 10.1109/ACCESS.2019.2918640*

# A Conformal Split-Ring Loop as a Self-Resonator for Wireless Power Transfer

**JINGCHEN WANG[1], MARK PAUL LEACH[1], ENG GEE LIM[1], (Senior Member, IEEE), ZHAO WANG[1], ZHENZHEN JIANG[1], RUI PEI[1], AND YI HUANG[2], (Senior Member, IEEE)**

[1]Department of Electrical and Electronics Engineering, Xi'an Jiaotong-Liverpool University, Suzhou 215123, China
[2]Department of Electrical Engineering and Electronics, University of Liverpool, Liverpool L69 3BX, U.K.

Corresponding author: Eng Gee Lim (enggee.lim@xjtlu.edu.cn)

This work was supported in part by the AI University Research Centre (AI-URC) through the XJTLU Key Programme Special Fund under Grant KSF-P-02, and in part by the XJTLU Research Development Fund under Grant PGRS-13-03-06, Grant RDF-14-03-24, and Grant RDF-14-02-48.

**ABSTRACT** A conventional printed spiral coil (PSC) has a self-resonant frequency and its equivalent circuit is a parallel inductor–capacitor (LC) circuit. It is desirable to use PSCs in wireless power transfer (WPT) applications; however, these are most commonly constituted by a series-primary and series- or parallel-secondary circuit. This paper proposes a printed conformal split-ring loop with the characteristic of a series LC circuit at its resonance frequency. Regarding the loop as a self-resonator, a magnetic-resonance coupled (MRC) WPT system with series-primary and secondary operating at 433 MHz in the industrial scientific and medical (ISM) band is presented. The maximum measured power transfer efficiency is 87.9% at a transfer distance of 22 mm, the best-reported result for such a configuration.

**INDEX TERMS** Wireless power transfer, split-ring resonators, printed spiral coils, near fields, magnetic resonance coupling.

## I. INTRODUCTION

Wireless power transfer (WPT) is increasingly prevalent and popular in the modern world; it has been widely applied in industrial areas (portable/wearable electronic devices and electric cars) [1]–[5] and medical applications (medical sensors and implanted devices) [6]–[8] to charge batteries without the inconvenience of using wires.

The magnetic resonance coupling (MRC) method for WPT has provoked widespread and profound interest due to its various advantages, since it was reported by Kurs *et al.* from the Massachusetts Institute of Technology in 2007, using self-resonant coils [9]. Wire coils are widely used in MRC based WPT [10]–[12] because of their high-quality factor ($Q$), however, they present technical difficulties in precise fabrication and mass production [13]. Furthermore, due to the typically large area occupied by the wire coils, they are normally applicable for use in large electronic devices such as electric cars. They are not usually appropriate for use in small electronic devices such as implantable medical devices, wireless sensors and devices with integrated circuit boards using micromachining technology. Alternatively, planar printed spiral coils (PSCs) are low-profile, low-cost and can have relatively small-dimensions. Additionally, planar PSCs offer higher geometrical manufacturing precision and have the potential to be integrated together with integrated circuits or within packages [14]. The ability to manufacture PSCs on flexible substrates means that they are suitable for use in wearable devices. There have been many PSC designs proposed for MRC based WPT featuring various shapes including circular, square and rectangular spiral coils [13], [15], [16].

Frequencies such as 0.3 MHz, 6.78 MHz and 13.56 MHz were considered in most recent works for WPT [17]. At these frequencies, coils with large inductances, up to uH, can be created allowing high quality factors to be achieved and power transfer distance increased into the centimeters or meter ranges due to the longer wavelengths of typically more than 10 m. As electromagnetic energy absorption in human tissues increases with frequency, for implantable applications, lower frequency bands are typically selected. However, as received power is proportional to the rate of change of the incident magnetic field, choosing a higher carrier frequency improves power transfer. Therefore, a compromise between

The associate editor coordinating the review of this manuscript and approving it for publication was Trivikram Rao Molugu.

power transfer and field penetration into the human body must be made.

Few works related to coils printed on PCB in the sub-GHz region have been published, as standard spiral coils printed on PCB have low inductances (nH) and are therefore unable to realize high power transfer efficiencies or large transfer distances. Also, matching networks for both the primary (transmit) and secondary (receive) circuits are essential in achieving a high power transfer efficiency.

The equivalent circuit of a conventional PSC is a parallel LC network hence using a pair to form a WPT system would constitute a parallel-primary and parallel-secondary system. However, the parallel-parallel topology offers poor power transfer performance, since the voltage source would be loaded by an open circuit at resonance if directly connected [18]. The series-primary, series-secondary topology and the series-primary, parallel-secondary topology are most typically used for wireless power transfer.

In this work, a conformal planar split-ring loop is proposed with the characteristic of a series LC circuit. Importantly, this planar split-ring loop can be regarded as a self-resonator and is designed for use at 433 MHz. The proposed loop is a good candidate for WPT in applications such as Ultra High Frequency Radio Frequency Identification (UHF-RFID), for example in mobile devices where only the addition of the coil would be needed. In comparison to other work, the proposed system offers improved power transfer efficiency over a transfer distance of 22 mm (less than 0.05 of a wavelength). The design of the proposed split-ring loop is explained in Section II. The WPT performance is presented in Section III. The measurement setup and results are illustrated in Section IV and conclusions are provided in Section V.

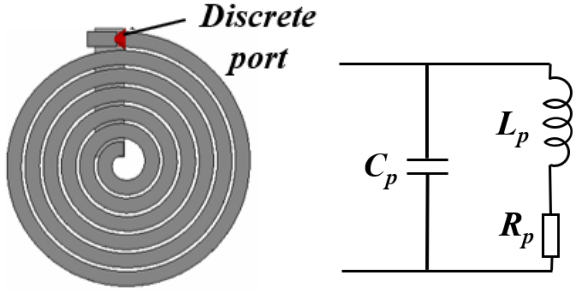


**FIGURE 1.** (a) Physical layout model of conventional 6-turn PSC. (b) The equivalent circuit of conventional 6-turn PSC.

## II. DESIGNS OF PLANAR SPLIT-RING LOOPS

A conventional PSC with 6 turns on FR-4 substrate ($\varepsilon_r = 4.4$) with a thickness of 1.5 mm, is shown in Figure 1(a). The width of each track is 2 mm and the gap between the two tracks is 0.5 mm. A discrete 50 Ω port was used for simulations. The equivalent circuit of the PSC is shown in in Figure 1(b). The real and imaginary parts of the impedance ($Z$) are shown in Figure 2. This conventional PSC is inductive at lower

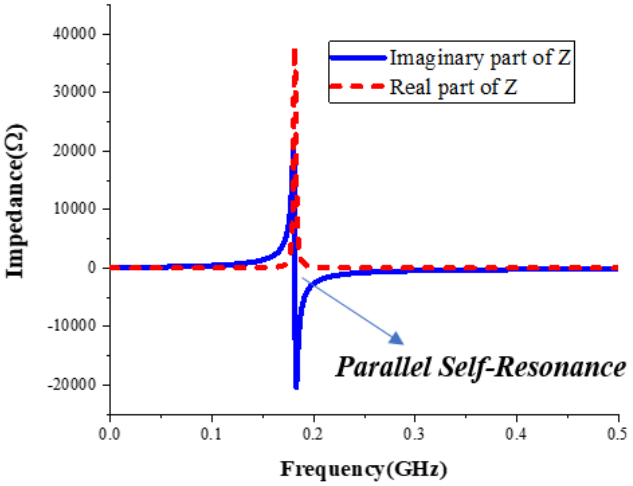


**FIGURE 2.** The equivalent circuit of conventional 6-turn PSC.

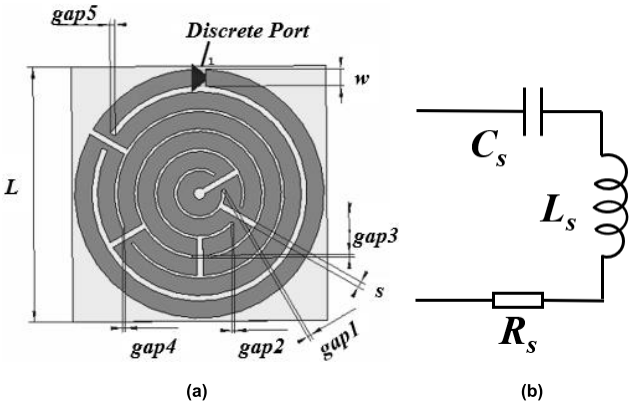


**FIGURE 3.** (a) Physical layout model of designed loop. (b) The equivalent circuit of designed sprit-ring loop at resonance frequency.

frequencies and becomes capacitive at higher frequencies. At the self-resonant frequency, the parallel LC circuit becomes open circuit (termed parallel self-resonance from this point), which as mentioned is not suitable for the primary side of the WPT system.

A conformal split-ring loop with small dimensions was designed in this work using the roundabout technique, as shown in Figure 3(a), in order to realize the characteristics of a series LC circuit at the desired frequency. The loop impedance was optimized by forcing **Im**($Z$) to zero and minimizing **Re**($Z$) at 433 MHz. This was achieved by setting *gap5* to 0.5 mm and then sweeping parameter *w* from 2 mm to 3.5 mm. A second optimization stage then swept *gap5* from 0.5 mm to 2 mm, as shown in Figure 4 and Figure 5 respectively.

It can be seen in Figure 4 that each curve has two parallel self-resonances and an additional point exists between these two where the loop acts as a series LC circuit (as shown in Figure 3(b)), indicated by the impedance changing from capacitive to inductive with increasing frequency (termed

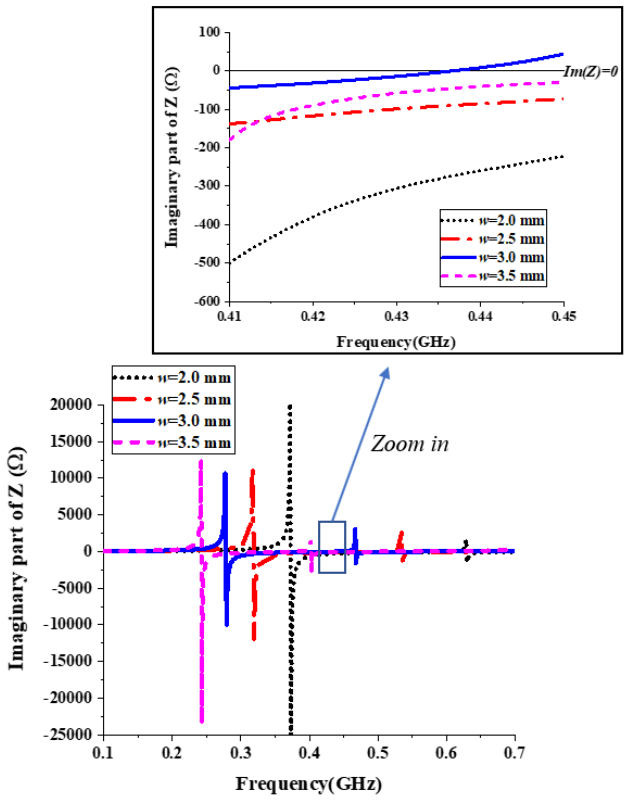


**FIGURE 4.** The imaginary part of impedance of designed loop antenna with the varying of frequency by changing the width of each track.

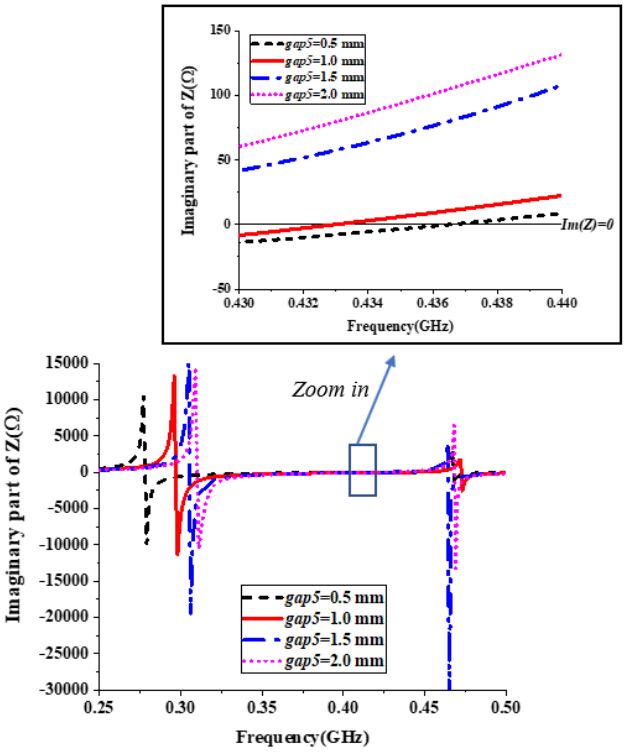


**FIGURE 5.** The equivalent impedance of designed loop antenna with the varying of frequency by changing the parameter of *gap5*.

series self-resonance from this point). Only when the parameter $w$ is 3 mm, does the series self-resonant point exist around 433 MHz.

The parameter *gap5* was optimized by varying as 0.5 mm, 1 mm, 1.5 mm and 2 mm to bring the series self-resonant point closer to 433 MHz. From Figure 5, it is worth noting that varying *gap5* results in a shifting of the parallel self-resonances, they shift closer together as *gap5* increases.

The imaginary part of the impedance of this split-ring loop is greater than zero in the frequency range of interest when the parameter *gap5* is 1.5 mm and 2.0 mm. When *gap5* is equal to 1.0 mm the imaginary part of the impedance at 433 MHz is closest to zero.

The details of the final optimized parameters for this split-ring loop are provided in TABLE 1. The thickness of the FR-4 substrate is 1.5 mm. The equivalent impedance of the designed split-ring loop is shown in Figure 6. It can be seen from Figure 6 that the simulated imaginary part of the impedance is almost zero at 433 MHz. Therefore, this proposed split-ring loop can be considered as a self-resonator with one series self-resonant frequency of 433 MHz. The real part of the impedance of the proposed split-ring loop is very large at the two parallel self-resonances, whereas the real part of the impedance is only 1.04 Ω at the series self-resonance point.

All optimizations are by means of full-wave simulations performed using the transient solver of Computer Simulation

**TABLE 1.** Dimensions of the proposed split-ring loop (units: mm).

| Parameter | Value | Parameter | Value |
|---|---|---|---|
| $L$ | 45 | $w$ | 3.0 |
| *gap1* | 0.5 | *gap2* | 0.5 |
| *gap3* | 0.5 | *gap4* | 0.5 |
| *gap5* | 1.0 | $s$ | 1.0 |

Technology (CST) Microwave Studio. According to previous parameter optimizations, the width of each trace has a significant influence on the self-resonance frequency, whereas, the gap between adjacent traces has little influence. Consequently, the optimization procedure to obtain a specific series self-resonance frequency can be summarized as follows. Firstly, initial values for $w$, $s$ and the various trace *gap* parameters should be set. Secondly, the width of each trace should be swept until the series self-resonance frequency is close to the frequency of interest. Final optimization is achieved by sweeping the value of each gap parameter between adjacent traces to achieve series self-resonance at the frequency of interest.

## III. PLANAR SPLIT-RING LOOPS AS SELF-RESONTORS FOR WIRELESS POWER TRANSFER

### A. THE PERFORMANCE OF WIRELESS POWER LINK

For wireless power transfer, two resonant objects of the same resonant frequency conduct power exchange at that resonant frequency, which is magnetic resonance coupled wireless

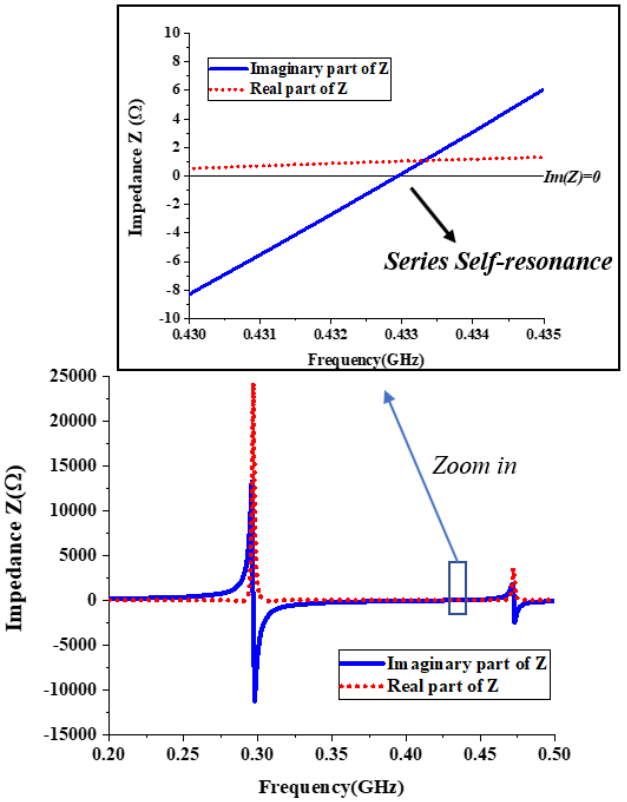


**FIGURE 6.** The equivalent impedance of designed split-ring loop with the varying of frequency.

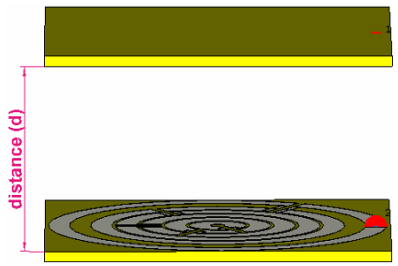


**FIGURE 7.** 3-D view of wireless power transfer.

power transfer. Two proposed split-ring loops with the same self-resonant frequency are used to constitute a WPT system of series-primary and series-secondary circuits. Two identical split-ring loops can be used as the Tx and Rx, respectively. A 3-D view of the loop as applied in WPT is shown in Figure 7. The distance between Tx and Rx is 25 mm.

The simulated scattering parameters of the final loop design are shown in Figure 8 for a fixed distance of 25 mm between the Tx and Rx loops. A reference impedance of 50 Ω has been assumed at both ports. It can be seen from Figure 8 that the proposed antenna operates at 433 MHz covering a bandwidth of at least 27 MHz (421-448 MHz) for $S_{11} < -10$ dB, which covers the 433-434 MHz ISM (Industrial Scientific Medical) band. Additionally, at 433 MHz, the scattering parameters are $|S_{11}| = -24.04$ dB, $|S_{21}| = -0.74$ dB, and $|S_{22}| = -23.9$ dB.

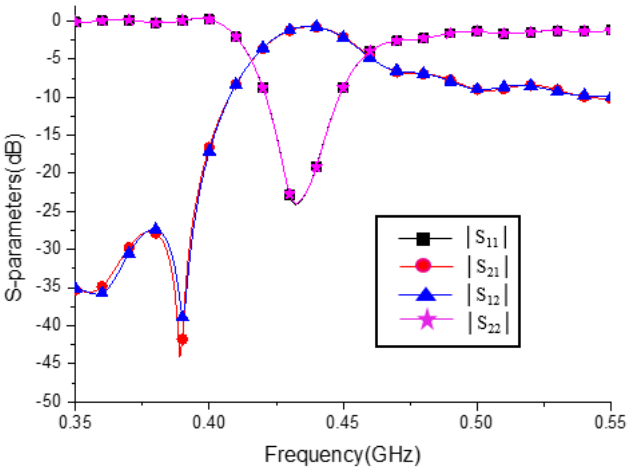


**FIGURE 8.** Simulated scattering parameters of proposed antennas for wireless power transfer.

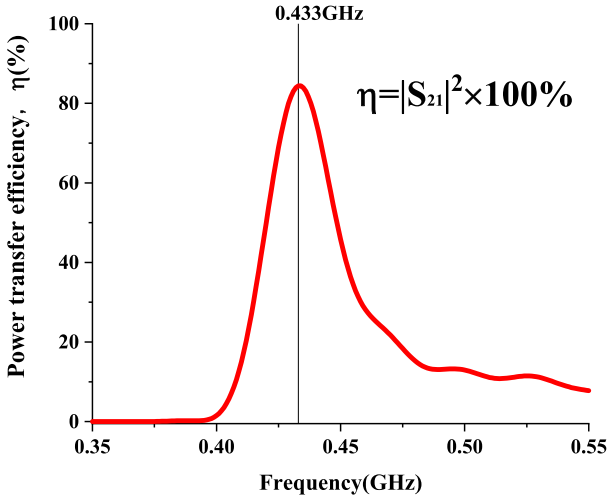


**FIGURE 9.** Simulated power transfer efficiency between two proposed antennas for wireless power transfer with the distance of 25 mm.

Both source impedance ($Z_{in}$) and load impedance ($Z_{Load}$) are designed to be 50 Ω, to allow practical measurements of the power transfer efficiency ($\eta$) between the split-ring loops obtained using [19]:

$$\eta = \frac{Power\ delivered\ to\ the\ load\ Z_{\mathrm{Load}}}{Available\ power\ from\ the\ source} = |S_{21}|^2 \times 100\% \quad (1)$$

The trend of power transfer efficiency against frequency is shown in Figure 9. It can be seen that the peak of the power transfer efficiency is 84.33% at 433 MHz. The power transfer efficiency is over 80% over the frequency band 430 MHz to 440 MHz, and hence is not highly sensitive to operating frequency shift. However, the power transfer efficiency dramatically decreases to 40% from 80% within narrow bands from 417 MHz to 430 MHz and from 440 MHz to 455 MHz. In other words, the power transfer efficiency reaches its maximum at the resonant frequency (433 MHz), then decreases greatly within a narrow band.

### B. PARAMETERS ANALYSIS

The influence of the split-ring loop's series self-resonant frequency on maximum power transfer efficiency has been investigated. The parameters *w* and *gap5* were swept again to obtain plots of simulated power transfer efficiency over the same ranges of the parameters used previously.

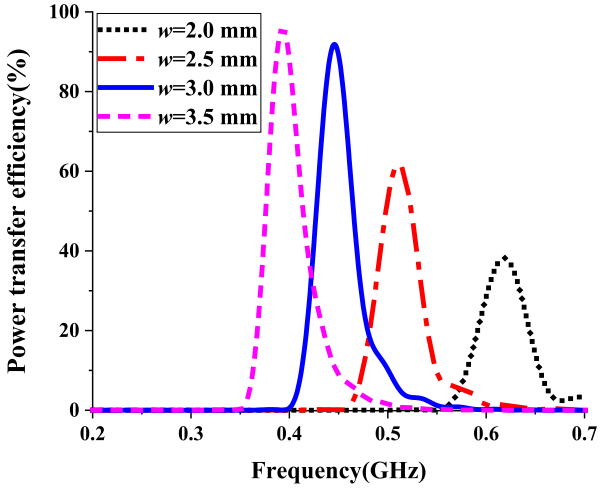


**FIGURE 10.** Simulated power transfer efficiency of proposed split-ring loop for wireless power transfer in dB by changing of the parameter *w*.

Figure 10 shows the simulated power transfer efficiency for variation in parameter *w* (with *gap5* fixed at 0.5 mm). It is clear to see from Figure 10 that the parameter *w* has a great influence on the loop self-resonant frequency at which the power transfer efficiency reaches its peak. The resonant frequency decreases as parameter *w* increases, which can also be inferred from Figure 4.

Even though the power transfer efficiency of each curve reaches a peak at the resonant frequency, the maximum power transfer efficiency of each curve is not always over 80%. The main reason for this is that for MRC the power transfer efficiency is dependent on the mutual inductance of the loops, which is distance dependent and changes with the width of the track *w*. Therefore, each antenna will have its own optimal distance based on the loop inductance at the operating frequency.

Figure 11 shows the simulated power transfer efficiency for variation in parameter *gap5* (with *w* fixed at 3 mm). It can be seen that the parameter *gap5* has little influence on the resonant frequency where the power transfer efficiency has its peak value. This is because *gap5* has little influence on the series self-resonant frequency where the zero crossings of the imaginary part of the impedance are closer together than for *w* variation, as also shown in Figure 5. The resonant frequency where the power transfer efficiency reaches a peak is inversely proportional to the value of the parameter *gap5*.

The maximum power transfer efficiency of each curve is over 80%, whereas the power transfer efficiency is highest at 433 MHz when the parameter *gap5* is 1 mm. Variation in the

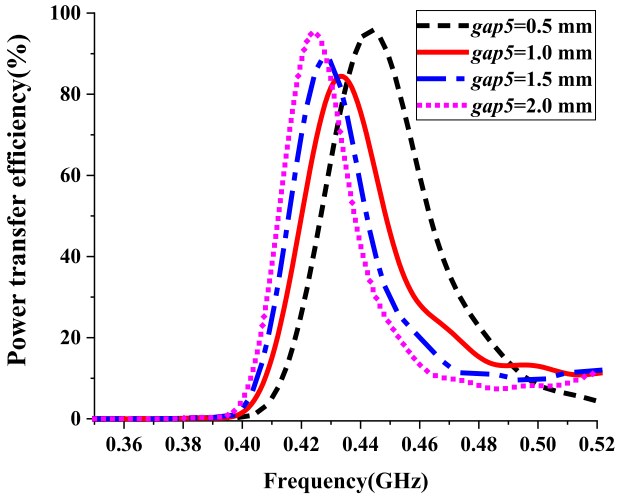


**FIGURE 11.** Simulated power transfer efficiency of proposed split-ring loop for wireless power transfer in dB by changing of the parameter *gap5*.

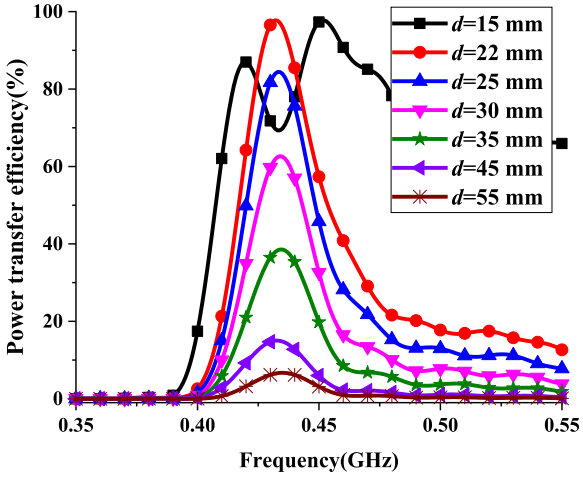


**FIGURE 12.** Simulated power transfer efficiency for different transfer distances.

*gap5* parameter effects the resistance and inductance of the loop. The change in resistance results in a variation in maximum power transfer efficiency through increased mismatch and losses. Changes in inductance lead to the same situation as for varying parameter *w*, in which power transfer efficiency is related to the transfer distance due to the mutual inductance of the antennas.

### C. EFFECTS OF TRANSFER DISTANCE

The effect of transfer distance on WPT performance should be considered in taking measurements and in designing practical applications. The transfer distance *d* relates to the distance between Tx and Rx, as shown in Figure 7. The transfer distances investigated by simulation are 15 mm, 22 mm, 25 mm, 30 mm, 35 mm, 45 mm and 55 mm. The power transfer efficiency can be calculated by equation (1) for each transfer distance, as shown in Figure 12.

It is worth noting that the simulated power transfer efficiency reaches its peak of 95.7% at a transfer distance of 22 mm. The power transfer efficiency decreases significantly from 95.7% to 5% as the transfer distance increases from 22 mm to 55 mm, which results from the coupling coefficient decreasing exponentially with increasing transfer distance. The power transfer efficiency remains at over 50% up to transfer distances of less than 30 mm. When the transfer distance is 15 mm, the power transfer efficiency has two peaks, one at 420 MHz and the other at 452 MHz, respectively, which results from the frequency splitting phenomena [20]. The power transfer efficiency is 66.33% at 433 MHz, which is not at a peak and is less than that at the transfer distance of 25 mm. Therefore, in general, power transfer efficiency between two antennas reaches a peak at a certain transfer distance.

## IV. MEASUREMENT SETUP AND RESULTS

The proposed antenna was fabricated on FR-4 substrate as shown in Figure 13(a) using a PCB milling machine. Figure 13(b) shows the measurement setup, where a Vector Network Analyzer (VNA) is used with a reference impedance of 50 Ω. The two antennas are directly soldered with subminiature version A (SMA) connectors and then connected to two VNA ports, respectively.

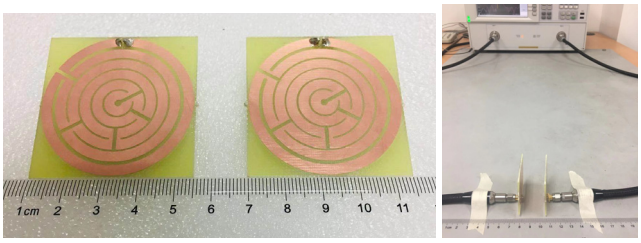


(a) (b)

**FIGURE 13.** (a) Fabricated antennas. (b) Measurement of proposed antennas for wireless power transfer.

The measured scattering parameters are shown in Figure 14, in which a slight frequency shift is seen to exist between the simulation and measurement results. The value of $S_{11}$ drops below −10 dB over a smaller frequency range, from 425 MHz to 445 MHz, but the proposed antenna still has enough bandwidth to cover the MedRadio band and the 433-434 MHz ISM band. At 433 MHz, the values of measured $|S_{11}|$, $|S_{21}|$, $|S_{22}|$ are −16.2 dB, −1.03 dB and −17.9 dB, respectively. Overall, the measured results show good agreement with the simulated results.

The self-resonance of the antenna relies on the parasitic capacitance formed between the conductive tracks of the loop; therefore, it is necessary to consider possible effects of surrounding mediums on the capacitance value that would lead to a shift in resonance frequency. Practical scenarios in which non-metallic mediums such as plastic, foam and paper are placed in the direct vicinity of, as well as in between,

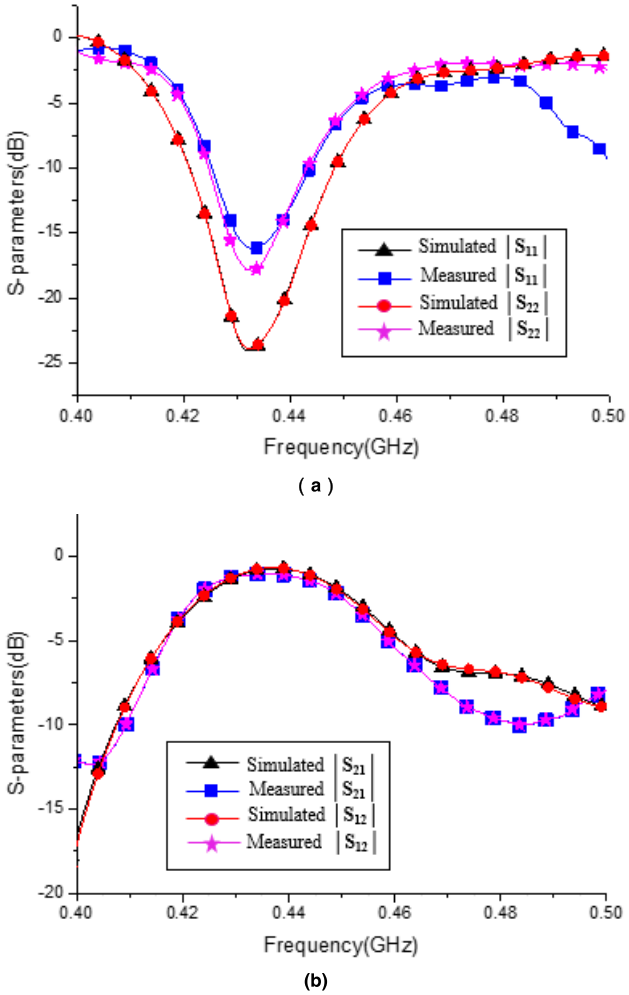


**FIGURE 14.** Simulated and measured scattering parameters of proposed antennas for wireless power transfer (a) reflection coefficient in dB (b) transmission coefficient in dB.

the Tx and Rx resonators have been investigated. The performance of wireless power transfer is not visibly affected by the presence of these external subjects. A similar process was followed using metal materials such as copper sheet, which was also seen to have no clear influence on performance even within several millimeters of the resonators.

The trends of numerical and experimental power transfer efficiency against transfer distance are shown in Figure 15. It can be observed from Figure 15 that the numerical and experimental power transfer efficiency first increases and then decreases greatly as the transfer distance rises from 15 mm to 55 mm at 433 MHz. This initially lower efficiency over shorter distances is due to the frequency splitting phenomenon [20].

The measured power transfer efficiency is seen to be lower than seen in the simulation results. The first reason for this is due to axis misalignment or rotation of the transmitter with respect to the receiver during experiments. What's more, the parasitic resistance of the fabricated loop (typically larger)

**TABLE 2. Comparisons of this antenna with other work.**

| Ref. | Types | $f_0$ (MHz) | Tx Size (mm) | Rx Size (mm) | Transfer Distance (mm) | Simulated PTE | Measured PTE |
|---|---|---|---|---|---|---|---|
| [21] | Rectangular coils on PCB | 110 | 10×10 | 10×10 | 3 (0.0011λ) | 30% | / |
| [22] | Square Printed Spiral Coils | 50.25 | 120×120 | 120×120 | 100 (0.01675λ) | / | 43.62% |
| [23] | H-slot Resonators | 1450 | 20×20 | 20×20 | 3.5 (0.01692λ) | 90% | 85% |
| This work | Planar Split-ring Resonators | 433 | 45×45 | 45×45 | 22 (0.03175λ) | 95.7% | 87.9% |

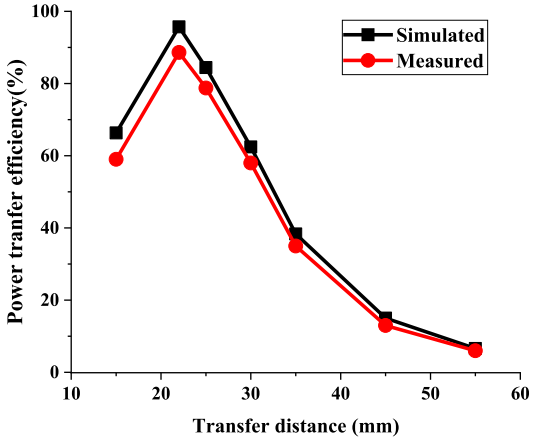


**FIGURE 15. Simulated and measured power transfer efficiency of proposed antennas for wireless power transfer against transfer distance.**

is different to that of the simulation due to material tolerances and fabrication errors. This extra resistance results in additional losses. Even though the measured power transfer efficiency is not as high as in the simulated results, the power transfer efficiency is still high at 78.77% over a transfer distance of 25 mm and 87.9% over a transfer distance of 22 mm.

Comparisons of this design with other works are summarized in TABLE 2. This proposed split-ring loop can be used for wireless power transfer in the UHF band. Despite the relatively large size, the split-ring loop can achieve higher power transfer efficiency over a larger transfer distance at a higher frequency than in other works. Additionally, the power transfer efficiency remains at over 30% when the transfer distance increases to 35 mm, which is also better performance than in the other published works, especially at 433 MHz.

## V. CONCLUSION

A conformal split-ring loop has been introduced and discussed in this paper. The loop has the characteristic of a series LC resonant circuit at one of its self-resonant frequencies, indicated by the imaginary part of the impedance curve changing from capacitive to inductive with increasing frequency. The series LC looks like a small resistance at the resonance frequency. The loop is designed to resonate at 433 MHz (UHF band) without the need for additional matching circuits, which makes the system simpler, more compact and easily adaptable for use in many WPT applications where space is restricted and complexity needs to be avoided. The performance of the WPT system, was measured, resulting in a power transfer efficiency reaching 87.9% at a transfer distance of 22 mm. In comparison with existing literature, this proposed design has the advantages of easy fabrication, smaller size, and longer transmission distances at similar efficiencies. The measured results show good agreement with the simulated results and demonstrate that the proposed split-ring loop antenna is a good candidate for WPT as a self-resonant structure for applications such as portable or mobile devices with RFID functions.

## ACKNOWLEDGMENT

The authors would like to express their sincere gratitude to CST AG for providing the CST STUDIO SUITE® electromagnetic simulation software package under the China Key University Promotion Program and Suzhou Municipal Key Lab for Wireless Broadband Access Technologies in the Department of Electrical and Electronics Engineering, Xi'an Jiaotong-Liverpool University, for research facilities.

## REFERENCES

[1] R. Wu, W. Li, H. Luo, J. K. Sin, and C. P. Yue, "Design and characterization of wireless power links for brain–machine interface applications," *IEEE Trans. Power Electron.*, vol. 29, no. 10, pp. 5462–5471, Oct. 2014.

[2] C. Liu, K. T. Chau, Z. Zhang, C. Qiu, W. Li, and T. Ching, "Wireless power transfer and fault diagnosis of high-voltage power line via robotic bird," *J. Appl. Phys.*, vol. 117, no. 17, 2015, Art. no. 17D521.

[3] D. H. Tran, Van B. Vu, and W. Choi, "Design of a high-efficiency wireless power transfer system with intermediate coils for the on-board chargers of electric vehicles," *IEEE Trans. Power Electron.*, vol. 33, no. 1, pp. 175–187, Jan. 2018.

[4] M. Bojarski, E. Asa, K. Colak, and D. Czarkowski, "Analysis and control of multiphase inductively coupled resonant converter for wireless electric vehicle charger application," *IEEE Trans. Transport. Electrific.*, vol. 3, no. 2, pp. 312–320, Jun. 2017.

[5] K. Hwang, J. Cho, D. Kim, J. Park, J. K. Kwon, S. I. Kwak, H. H. Park, and S. Ahn, "An autonomous coil alignment system for the dynamic wireless charging of electric vehicles to minimize lateral misalignment," *Energies*, vol. 10., no. 3, p. 315, 2017.

[6] T. Campi, S. Cruciani, F. Palandrani, V. De Santis, A. Hirata, and M. Feliziani, "Wireless power transfer charging system for AIMDs and pacemakers," *IEEE Trans. Microw. Theory Techn.*, vol. 64, no. 2, pp. 633–642, Feb. 2016.

[7] K. Na, H. Jang, H. Ma, and F. Bien, "Tracking optimal efficiency of magnetic resonance wireless power transfer system for biomedical capsule endoscopy," *IEEE Trans. Microw. Theory Techn.*, vol. 63, no. 1, pp. 295–304, Jan. 2015.

[8] G. Xu, X. Yang, Q. Yang, J. Zhao, and Y. Li, "Design on magnetic coupling resonance wireless energy transmission and monitoring system for implanted devices," *IEEE Trans. Appl. Supercond.*, vol. 26, no. 4, Jun. 2016, Art. no. 4400804.
[9] A. Kurs, A. Karalis, R. Moffatt, J. D. Joannopoulos, P. Fisher, and M. Soljacic, "Wireless power transfer via strongly coupled magnetic resonance," *Science*, vol. 317, no. 5834, pp. 83–86 Jul. 2007.
[10] A. K. RamRakhyani, S. Mirabbasi, and M. Chiao, "Design and optimization of resonance-based efficient wireless power delivery systems for biomedical implants," *IEEE Trans. Biomed. Circuits Syst.*, vol. 5, no. 1, pp. 48–63, Feb. 2011.
[11] H. Hu and S. V. Georgakopoulos, "Multiband and broadband wireless power transfer systems using the conformal strongly coupled magnetic resonance method," *IEEE Trans. Ind. Electron.*, vol. 64, no. 5, pp. 3595–3607, May 2017.
[12] C.-C. Huang, C.-L. Lin, and Y.-K. Wu, "Simultaneous wireless power/data transfer for electric vehicle charging," *IEEE Trans. Ind. Electron.*, vol. 64, no. 1, pp. 682–690, Jan. 2017.
[13] F. Jolani, Y. Yu, and Z. Chen, "A planar magnetically coupled resonant wireless power transfer system using printed spiral coils," *IEEE Antennas Wireless Propag. Lett.*, vol. 13, pp. 1648–1651, 2014.
[14] U.-M. Jow and M. Ghovanloo, "Modeling and optimization of printed spiral coils in air, saline, and muscle tissue environments," *IEEE Trans. Biomed. Circuits Syst.*, vol. 3, no. 5, pp. 339–347, Oct. 2009.
[15] S. Hekal, A. B. Abdel-Rahman, H. Jia, A. Allam, A. Barakat, T. Kaho, and R. K. Pokharel, "Compact wireless power transfer system using defected ground bandstop filters," *IEEE Microw. Wireless Compon. Lett.*, vol. 26, no. 10, pp. 849–851, Oct. 2016.
[16] C. Xiao, Y. Liu, D. Cheng, and K. Wei, "New insight of maximum transferred power by matching capacitance of a wireless power transfer system," *Energies*, vol. 10, no. 5, p. 688, May 2017.
[17] A. Christ, M. Douglas, J. Nadakuduti, and N. Kuster, "Assessing human exposure to electromagnetic fields from wireless power transmission systems," *Proc. IEEE*, vol. 101, no. 6, pp. 1482–1493, Jun. 2013.
[18] J. Wang, M. Leach, E. G. Lim, Z. Wang, and Y. Huang, "Investigation of magnetic resonance coupling circuit topologies for wireless power transmission," *Microw. Opt. Technol. Lett.*, vol. 61, no. 7, pp. 1755–1763, 2019.
[19] V. Talla and J. R. Smith, "An experimental technique for design of practical wireless power transfer systems," in *Proc. IEEE Int. Symp. Circuits Syst.*, Melbourne, VIC, Australia, Jun. 2014, pp. 2041–2044.
[20] A. P. Sample, D. T. Meyer, and J. R. Smith, "Analysis, experimental results, and range adaptation of magnetically coupled resonators for wireless power transfer," *IEEE Trans. Ind. Electron.*, vol. 58, no. 2, pp. 544–554, Feb. 2011.
[21] S. Kim, B. Bae, S. Kong, D. H. Jung, J. J. Kim, and J. Kim, "Design, implementation and measurement of board-to-board wireless power transfer (WPT) for low voltage applications," in *Proc. IEEE 22nd Conf. Elect. Perform. Electron. Packag. Syst.*, Oct. 2013, pp. 91–95.
[22] M. M. Falavarjani, M. Shahabadi, and J. Rashed-Mohassel, "Design and implementation of compact WPT system using printed spiral resonators," *Electron. Lett.*, vol. 50, no. 2, pp. 110–111, Jan. 2014.
[23] S. Hekal, A. B. Abdel-Rahman, H. Jia, A. Allam, R. K. Pokharel, and H. Kanaya, "Strong resonant coupling for short-range wireless power transfer applications using defected ground structures," in *Proc. IEEE Wireless Power Transf. Conf.*, Boulder, CO, USA, May 2015, pp. 1–4.

**JINGCHEN WANG** received the B.Eng. and M.Eng. degrees in electrical and information engineering from Xi'an Jiaotong University, Xi'an, China, in 2011 and 2013, respectively. She is currently pursuing the Ph.D. degree in wireless communications and RF engineering with the University of Liverpool, Liverpool, U.K.

Her research interests include wearable antennas, implantable antennas, wireless power transfer, and energy harvesting. She has been a Reviewer of the IEEE TRANSACTIONS ON ANTENNAS AND PROPAGATION.

**MARK PAUL LEACH** received the B.Eng. degree (Hons.) in communication and electronic engineering and the Ph.D. degree from the University of Northumbria, U.K., in 1999 and 2005, respectively.

From 2003 to 2008, he was a Research Associate in microwave holography. From 2008 to 2013, he was a Lecturer with the Seoul National University of Science and Technology, conducting research into thin films for photovoltaic applications. In 2013, he joined as an Associate Professor with the Department of Electrical and Electronic Engineering, Xi'an Jiaotong-Liverpool University. His current research interests include antennas, RF/microwave engineering, EM measurements/simulations, energy harvesting, wireless power/energy transfer, and wireless communication networks.

**ENG GEE LIM** (Senior Member, IEEE) received the B.Eng. (Hons.) and Ph.D. degrees in electrical and electronic engineering from the University of Northumbria, U.K.

From 2002 to 2007, he worked with Andrew Ltd., a leading communications systems company in U.K. Since August 2007, he has been with Xian Jiaotong-Liverpool University, where he was formally the Head of the EEE Department and the University Dean of Research and Graduate studies. He is currently the Director of AI University Research Centre and also a Professor with the Department of Electrical and Electronic Engineering. He has published over 100 refereed international journals and conference papers. His research interests are artificial intelligence, robotics, AI+ health care, International Standard (ISO/ IEC) in robotics, antennas, RF/microwave engineering, EM measurements/simulations, energy harvesting, power/energy transfer, smart-grid communication, and wireless communication networks for smart and green cities. He is also a charter Engineer, Fellow of IET, and Senior Fellow of HEA.

**ZHAO WANG** received the B.Eng. degree in electronic and information engineering from Xi'an Jiaotong University, China, in 2003, and the Ph.D. degree in wireless communication and electromagnetics from the Queen Mary University of London, U.K., in 2009.

She has been with the Department of Electrical and Electronics Engineering, Xi'an Jiaotong-Liverpool University, where she is currently an Associate Professor, since 2010. Her research interests include antennas and the optimization algorithms, RF & microwave engineering, energy harvesting, wireless power transfer, and robotics.

**ZHENZHEN JIANG** was born in Henan, China, in 1994. She received the B.Eng. degree (Hons.) in telecommunication engineering from Xi'an Jiaotong-Liverpool University, Suzhou, China, in 2016. She is currently pursuing the Ph.D. degree in wireless communications and RF engineering with the University of Liverpool, Liverpool, U.K.

Her research interests include implantable antenna design, simultaneously wireless power and data transfer, energy harvesting, and rectifying circuit.

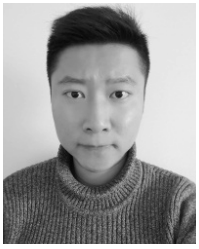

**RUI PEI** was born in Wuhu, China, in 1993. He received B.Eng. degree (Hons.) from Xi'an Jiaotong-Liverpool University and the University of Liverpool, in 2015, and the M.Sc. degree (Hons.) from the University of Edinburg, in 2016. He is currently pursuing the Ph.D. degree with the University of Liverpool and Xi'an Jiaotong-Liverpool University, Suzhou, China.

His research interests include antenna design, wearable antennas, specific absorption rate, and body area networks.

**YI HUANG** (S'91–M'96–SM'06) received the B.Sc. degree in physics from Wuhan University, Wuhan, China, in 1984, the M.Sc. (Eng.) degree in microwave engineering from the Nanjing Research Institute of Electronics (NRIET), Nanjing, China, in 1987, and the D.Phil. degree in communications from the University of Oxford, Oxford, U.K., in 1994.

He was a Radar Engineer with NRIET and a Member of Research Staff with the University of Birmingham, Birmingham, U.K., the University of Oxford, Oxford, U.K., and the University of Essex, Colchester, U.K. In 1994, he joined the British Telecom Labs, as a Research Fellow. In 1995, he joined as a Faculty Member with the Department of Electrical Engineering and Electronics, University of Liverpool, Liverpool, U.K., where he is currently a Full Professor in wireless engineering, the Head of the High Frequency Engineering Group, and the Deputy Head of the Department. Since 1987, he has been involved in wireless communications, applied electromagnetics, radar, and antennas. He has authored over 300 refereed papers in leading international journals and conference proceedings, and authored *Antennas: From Theory to Practice* (Wiley, 2008) and *Reverberation Chambers: Theory and Applications to EMC, and Antenna Measurements* (Wiley, 2016).

Dr. Huang is a Senior Fellow of the HEA and a Fellow of the IET. He received many research grants from research councils, government agencies, charity, EU, and industry, acted as a consultant to various companies, and served on a number of the national and international technical committees and has been an Editor, and an Associate Editor, or a Guest Editor of four international journals. He has been a keynote/Invited Speaker and an Organizer of many conferences and workshops (e.g., WiCom 2006, 2010, the IEEE iWAT2010, and LAPC 2012). He is currently the Editor-in-Chief of *Wireless Engineering and Technology* and an Associate Editor of the IEEE Antennas and Wireless Propagation Letters, and the U.K. and Ireland Rep to the European Association of Antenna and Propagation.